ENVIRONMENTAL RESEARCH
LETTERS

LETTER • OPEN ACCESS

# Intensification of the dispersion of the global climatic landscape and its potential as a new climate change indicator

To cite this article: Yanlong Guan *et al* 2020 *Environ. Res. Lett.* **15** 114032

Environmental Research Letters

LETTER

# Intensification of the dispersion of the global climatic landscape and its potential as a new climate change indicator

Yanlong Guan[1,3,4], Hongwei Lu[2,1], Li He[3,1], Hari Adhikari[4], Petri Pellikka[4,6], Eduardo Maeda[4] and Janne Heiskanen[4,5]

[1] School of Renewable Energy, North China Electric Power University, Beijing, People's Republic of China
[2] Key Laboratory of Water Cycle and Related Land Surface Process, Institute of Geographic Science and Natural Resources Research, Chinese Academy of Science, Beijing, People's Republic of China
[3] State Key Laboratory of Hydraulic Engineering Simulation and Safety at Tianjin University, Tianjin, People's Republic of China
[4] Department of Geosciences and Geography, University of Helsinki, Helsinki, Finland
[5] Institute for Atmospheric and Earth System Research, Faculty of Science, University of Helsinki, Helsinki, Finland
[6] State Key Laboratory for Information Engineering in Surveying, Mapping and Remote Sensing, Wuhan University, Wuhan 430079, People's Republic of China

**E-mail:** luhw@igsnrr.ac.cn

**Keywords:** Köppen–Geiger climate classification, global climate landscape, dispersion, patch aggregation, global climate diversity

Supplementary material for this article is available online

OPEN ACCESS

RECEIVED
21 August 2019

REVISED
22 June 2020

ACCEPTED FOR PUBLICATION
3 July 2020

PUBLISHED
20 November 2020



## Abstract

Increases and decreases in the areas of climatic types have become one of the most important responses to climate warming. However, few attempts have been made to quantify the complementary relationship between different climate types or to further assess changes in the spatial morphology. In this study, we used different observed datasets to reveal a dispersion phenomenon between major global climate types in 1950–2010, which is significantly consistent with the increasing trend of global temperatures. As the standard deviation of the area of major climate zones strengthened in 1950–2010, the global climatic landscape underwent notable changes. Not only did the area change, but the shape of the overall boundary became regular, the aggregation of climatic patches strengthened, and the climatic diversity declined substantially. However, changes in the global climatic landscapes are not at equilibrium with those on the continental scale. Interpreting these climatic morphological indices can deepen our understanding of the redistribution response mechanisms of species to climate change and help predict how they will be impacted by long-term future climate change.

## 1. Introduction

Climate classification is a necessary step towards understanding the complex spatio-temporal interactions between different climatic variables or phenomenon. As different regions are either becoming warmer, cooler, drier, or wetter at different rates, a non-uniform global response to climate change can be anticipated. Multiple climate measurement methods are extensively used to categorise geographical regions with different hydrological or climatic designs (Wells *et al* 2004, Kottek *et al* 2006, Baker *et al* 2009, Meybeck *et al* 2013, Knoben *et al* 2018, Papagiannopoulou *et al* 2018). Data regarding the distribution of most species on Earth are lacking. Therefore, climate classification metrics are particularly useful for understanding the impacts of climate change on biomes (Burrows *et al* 2011, Sunday *et al* 2012, Garcia *et al* 2014).

An extensively used climate classification that was summarised by Köppen (1931) has been modified into different versions (Lee 1947, Thornthwaite 1948, 1961, Feddema 2005, Kottek *et al* 2006, Peel *et al* 2007). The Köppen climate classification links global surface climates and the qualitative characteristics of vegetation. This classification is based on the annual and monthly mean temperature and precipitation as an expression of vegetation. The association between climate and vegetation provides an easy-to-visualise empirical, and intuitive relationship between the multivariate descriptions of climate and the natural landscape. Although some complexities are excluded from the classification process, this classification is still widely used in the study of climate

and biomes because of its simplicity and useful features.

Previous climate measurement studies have analysed different climate classifications (Kottek *et al* 2006, Peel *et al* 2007, Papagiannopoulou *et al* 2018), spatial changes in climate types (Rubel and Kottek 2010, Feng *et al* 2014, Rohli *et al* 2015a), and the speed at which these changes occur (Burrows *et al* 2011, Mahlstein *et al* 2013). Furthermore, the availability of different gridded datasets allows for the diagnosis or projection of climate change by investigating the moving boundaries of the climate zone (Meybeck *et al* 2013, Phillips and Bonfils 2015, Beck *et al* 2018, Knoben *et al* 2018). However, these climatological metrics are not necessarily indicative of all the features of the climate spatio-temporal dynamics and their potential implications.

As with land cover classification, different climate zones have highly heterogeneous surface biophysical characteristics. However, the spatial heterogeneity assessment of the climate has not received extensive attention (Meybeck *et al* 2013). Furthermore, few attempts have been made to quantify the potential changes in spatial heterogeneity, through the lens of a climate zone. Species distribution models assume that the range of a species is fundamentally determined by climate (Burrows *et al* 2011, Sunday *et al* 2012, Garcia *et al* 2014). However, the spatial dynamics of climate heterogeneity can influence the capability of species to track suitable climatic conditions to maintain their niches. This results in communities re-arranging and has potential implications for species interacting and habitats changing (Sinervo *et al* 2010, Burrows *et al* 2011, Garcia *et al* 2014). The coverage of global cold climate zones is projected to shrink, while hot climate zones areas are more likely to expand due to temperature increases. The corresponding dynamics between increases and decreases are complementary during the period. Recent studies (Allen *et al* 2012, Liu and Allan 2013, Meybeck *et al* 2013, Mahlstein *et al* 2013, Rohli *et al* 2015a, Beck *et al* 2018) have shown that we can hypothesise the complementary relationship between major climate zone changes and global climate change. Therefore, this is an important indicator of climatic spatial morphology dynamics.

Landscapes consist of patches with relatively stable environmental conditions (Pickett and Cadenasso 1995). Spatial morphology allows for numerous landscape indices (Mcgarigal *et al* 2012) that can be used to describe the structural (i.e. connectivity) and functional (i.e. diversity) variation in a climatic landscape. These structural and functional measurements are primarily based on the assumption that the spatial heterogeneity of climatic patterns can strongly influence the range of species (Boucher-Lalonde *et al* 2012, Meybeck *et al* 2013, Carroll *et al* 2018). Furthermore, the assumed importance of these spatial patterns is related to structural and functional effects (Garcia *et al* 2014, Senf and Seidl 2018). Landscapes indicate that the complementary relationship of major climate zones provides an opportunity to explore the morphological characteristics of global climate zones as a whole.

This study quantifies the complementary relationship in the major climate zones along with using landscape indicators to explore long-term morphological changes in climatic landscapes on a global and continental scale. This was achieved by first evaluating the changes in the different climate zone areas based on the observed temperature and precipitation between 1950 and 2010. Thereafter, the standard deviation (SD) index was used to quantify the complementary relationships of major climate zones and to explain the dispersion variations of the global climatic landscape. An increase in the SD index between major climate zones is likely to cause significant responses across an entire landscape. Furthermore, we detected the changes in the area, shape, aggregation, and functional groups of climate landscapes. Finally, we examined the climatic variations on different continents to quantify the continental features of the climatic landscape. The morphological quantification of the climate types in this study can be used to improve the estimation of the unique climate change at a given scale. This can also better our understanding of the impacts of climate change on biomes.

## 2. Data and methods

### 2.1. Climate data

We collected monthly gridded precipitation and temperature datasets at 0.5° × 0.5° resolution from the University of East Anglia Climatic Research Unit (CRU TS V.4.02) (Harris *et al* 2014) and the University of Delaware Air Temperature & Precipitation (UD V5.01) (Willmott and Matsuura 2001). CRU TS V.4.02 provides a gridded time-series dataset based on observations from more than 4000 sites. The monthly average surface temperature and precipitation are included, among other variables, which serve as the basis of the climate classification scheme used in this work. CRU TS V.4.02 is applicable over land, excluding Antarctica, and covers the period between 1901 and 2017. UD V5.01 provides high-resolution gridded monthly station data for temperature and precipitation for the period of 1900 to 2014, with the dataset mainly relying on a large number of observations from the Global Historical Climate Network. In this study, we concentrate on the period of 1950 to 2010, and focus on global land, excluding Antarctica. As most previous studies (Kottek *et al* 2006, Spinoni *et al* 2015, Santini and Di Paola 2015, Rohli *et al* 2015a) concentrated on available datasets with a horizontal resolution of 0.5° to 2.5, the data sets used here were interpolated to a representative horizontal resolution of 1° following the bilinear method.

### 2.2. Köppen-Geiger climate classification

We used the Köppen-Geiger climate classification to generate the major annual climate types as described in (Peel *et al* 2007), which has also been widely used in different research fields (Greve *et al* 2014, Feng *et al* 2014, Almorox *et al* 2015, Chan and Wu 2015, Beck *et al* 2018). Overall, this climate scheme is consistent with the original version summarised by Köppen in 1936, but has some differences. For example, the −3 °C thresholds of temperate and cold climates are replaced with a 0 °C threshold, and arid climates are defined based on the occurrence of 70% precipitation during summer or winter. According to the updated climate classification scheme (Peel *et al* 2007), the first step is to identify arid climates, as any land pixel that meets the criteria of an arid climate may also meet the criteria of other climate types. The other main climate types are mutually exclusive as they are solely based on temperature thresholds (Feng *et al* 2014, Beck *et al* 2018). Before applying the climate classification algorithm, we used a 5-year running mean to reduce the adverse impacts of short-term climate variability and increase the robustness of the results (Mahlstein *et al* 2013). Shifts in climate zones over a 5-year average period are more likely to reflect signals caused by climate change, while interannual comparison would cause greater internal variability that may be unrelated to long-term climatic trends. Furthermore, SD was calculated based on the annual percentage area (PA) of each climate type to analyse the dynamics of the global climatic landscape. To validate the applicability of our results, we compared the maps over the period of 1976–2000 to the map generated by Kottek *et al* (2010) downloaded from http://koeppen-geiger.vu-wien.acat/shifts.htm. Climates A–E represent tropical, arid, temperate, cold, and polar climates, respectively (table S1 (available online at stacks.iop.org/ERL/15/114037/mmedia)).

### 2.3. Landscape analysis

The spatial patterns of the Köppen climate zones were quantitatively assessed using selected landscape indices to measure the characteristics at the landscape level. Different representations of space have led to the use of various spatial metrics to describe spatial structure and patterns. The public software FRAGSTATS version 4.2 was selected to conduct these spatial analyses (Mcgarigal *et al* 2012), which is widely used in many fields. Although FRAGSTATS provides a large number of spatial metrics, including the area, shape, aggregation, and diversity groups, many of them quantify similar or identical aspects of the landscape pattern. In most cases, the redundant metrics will have a high correlation and may even be perfectly correlated. In this study, we selected representative subsets that focus on different aspects at the landscape level, including the largest patch index (LPI) for area, landscape shape index (LSI) for shape (Cain *et al* 1997), contagion index (CONTAG) (O'Neill *et al* 1988), and aggregation index (AI) (He *et al* 2000) for aggregation, and Shannon's diversity index (SHDI) (Shannon 1948) and Simpson's diversity index (SIDI) (Simpson 1949) for diversity.

The LPI refers to the percentage of the total climatic landscape consisting of the largest climatic patch. LPI approaches 100 as the size of the largest patch in the landscape increases. The LPI for year $k$ ($LPI_k$) is calculated using the following equation:

$$LPI_k = \frac{Max(a_{ijk})}{A} \times 100 \quad (1)$$

where $Max(a_{ijk})$ denotes the maximum area of patch $j$ within climate zone $i$ (from 1 to $I$) in year $k$, and A is the total landscape area.

The LSI represents the total length of the edge of the climatic landscape, provided by the number of cell surfaces divided by the minimum possible total edge length. Thus, LSI increases as the landscape shape becomes more irregular. The LSI for year $k$ ($LSI_k$) is calculated as follows:

$$LSI_k = \frac{0.25e_k}{\sqrt{A}} \quad (2)$$

where $e_k$ denotes the total edge length $e$ in year $k$.

CONTAG is a measurement of the observed contagion over the maximum possible contagion for a specific number of climatic patch types. It is inversely related to the marginal density of climatic patches and has nothing to do with the specific distribution of climate types, such as coastal, or a type of climate surrounded by other climate types, such as EF and ET climates. Assuming that a single climatic class occupies a very large area of the landscape, the contagion is high when the edge density is very low, and approaches 100 when the patch types are maximally aggregated. For year $k$, $CONTAG_k$ is calculated as follows:

$$CONTAG_k = \left\{1 + \sum_{i=1}^{I}\sum_{f=1}^{I}\left[(P_{ik}) \times \left(g_{ifk}/\sum_{f=1}^{F} g_{ifk}\right)\right] \times \left[\ln(P_{ik}) \times \left(g_{ifk}/\sum_{f=1}^{F} g_{ifk}\right)\right]/2\ln(I)\right\} \times 100 \quad (3)$$

where variable $g_{ifk}$ denotes the number of adjacencies between the grids of climate zones $i$ and $f$ based on the double-count method in year $k$, $J_i$ represents the total number of patches in climate zone $i$, and $P_{ik}$ is the proportion of the landscape occupied by climate zone $i$ in year $k$.

The AI increases as the climatic landscape becomes more aggregated. For year $k$, $AI_k$ is calculated as follows:

$$AI_k = \left[\sum_{i=1}^{I}\left(\frac{g_{iik}}{\max - g_{iik}}\right) \times P_{ik}\right] \times 100 \quad (4)$$

where $g_{iik}$ denotes the number of similar adjacencies between the grids of climate zone $i$ based on the single-count method in year $k$, and $max\text{-}g_{iik}$ is the maximum number of similar adjacencies between the grids of climate zone $i$ based on the single-count method in year $k$. It increases as the number of different patch types increases and the proportional distribution of area between patch types becomes more homogenous.

The SHDI increases as the number of different patch categories increases and the proportional distribution of area among climatic patch categories becomes more homogenous. The value of $SHDI_K$ for year $k$ can be determined as follows:

$$SHDI_k = -\sum_{i=1}^{I}(P_{ik} \times \ln P_{ik}) \quad (5)$$

Another measure of diversity, the SIDI, represents the probability that any two pixels selected at random would be different patch categories. The SIDI in year $k$ ($SIDI_K$) is calculated as follows:

$$SIDI_k = 1 - \sum_{i=1}^{I} {P_{ik}}^2 \quad (6)$$

### 2.4. Statistical analysis

We applied the non-parametric Mann-Kendall statistical test (Mann 1945, Kendall 1975) to assess the statistical significance of the temporal climatic trend (Yue *et al* 2002). The M-K significance test is less affected by missing values and uneven distribution than other test methods. Generally, a $|Z|$ value of 1.96 is used to test for a 0.05 significance level. The null hypothesis is rejected if $|Z| > 1.96$. Additionally, the Pearson's correlation coefficient ($r$) was used to examine the statistical relationship between the SD index and landscape indices.

## 3. Results

### 3.1. Landscape changes in the global climate pattern

figure 1 shows the global distribution of climate types and the disappearing/emerging climate areas between 1950 and 2010. Although there are some distribution differences between the two versions due to the different data sets and thresholds, the results have a large overlap with the map drawn by (Rubel and Kottek 2010) (figure S1). The most notable feature is the expansion of arid B and tropical A climates in the Northern and Southern Hemispheres, respectively. In contrast, the polar E and temperate C climates in the Northern and Southern Hemispheres have shrunk greatly, respectively. As illustrated in figures 1(c) and (d), the climate zone shifts in the low and high latitudes exhibit a clear change in the polar direction, including areas such as Southern Brazil, Southern Sahara, and the Arctic. These changes may be attributed to increases in temperature at certain latitudes (Burrows *et al* 2011, Sunday *et al* 2012, Lu *et al* 2019). Additionally, the mid- and low-latitude high-altitude regions may be affected by climate change faster than their surrounding lowlands (such as central and southern Africa, the North American Rocky Mountains, South American Andes, and Tibetan Plateau). The reason for these changes may be changes in precipitation as mountainous areas are likely more affected by changes in precipitation than other regions (Mahlstein *et al* 2013). As illustrated in figure 2, the annual spatial pattern of the global climatic landscape was examined using representative landscape indices in 1950–2010. From a landscape perspective, the shape and diversity groups are significantly decreased, while the aggregation indices are significantly increased ($|Z| > 1.96$, MK) excluding the LPI. Overall, our results indicate that not only has the area changed, but the structural aggregation and functional diversity of the global climate landscape have also changed at the landscape level.

### 3.2. Intensification in the dispersion of global climatic landscape

We further calculated the PA and SD of major climatic zones to quantitatively analyse the evolution of the global landscape from 1950 to 2010 using the observed CRU datasets. As shown in figure 3(a), the annual cumulative PAs between the major climate types have changed relative to the starting values of 1950, while their SD anomalies have exhibited significant positive correlations with annual temperature (figure 3(c)) and precipitation (figure 3(e)); the increase in SD was more closely related to annual surface temperature increase ($r = 0.793$, $p < 0.01$) than precipitation ($r = 0.577$, $p < 0.01$). The PAs of the major climate zones (figure 3(a)) behaved as follows: tropical—0.074% decade$^{-1}$, arid—0.315% decade$^{-1}$, temperate—0.017% decade$^{-1}$, cold—0.029% decade$^{-1}$, and polar climates—0.442% decade$^{-1}$. Therefore, the differences in the area between the major climate types have become greater and the SD has significantly increased by 0.11% decade$^{-1}$. To further verify the relationship between the annual temperature and precipitation and the SD, we also calculated the PA and its corresponding SD trends using the UD datasets (figure 3(b)). The result revealed that the increase in temperature ($r = 0.696$, $p < 0.01$; figure 3(d)) is closer to the trends in SD, indicating that temperature plays a more important role in strengthening the SD anomaly than precipitation (figure 3(f)).

The changes in the global climatic landscape depend on the complementarity relationship of the area change of major climate types within the global climatic landscape. Therefore, the SD index calculated from major climate types can be used to explain

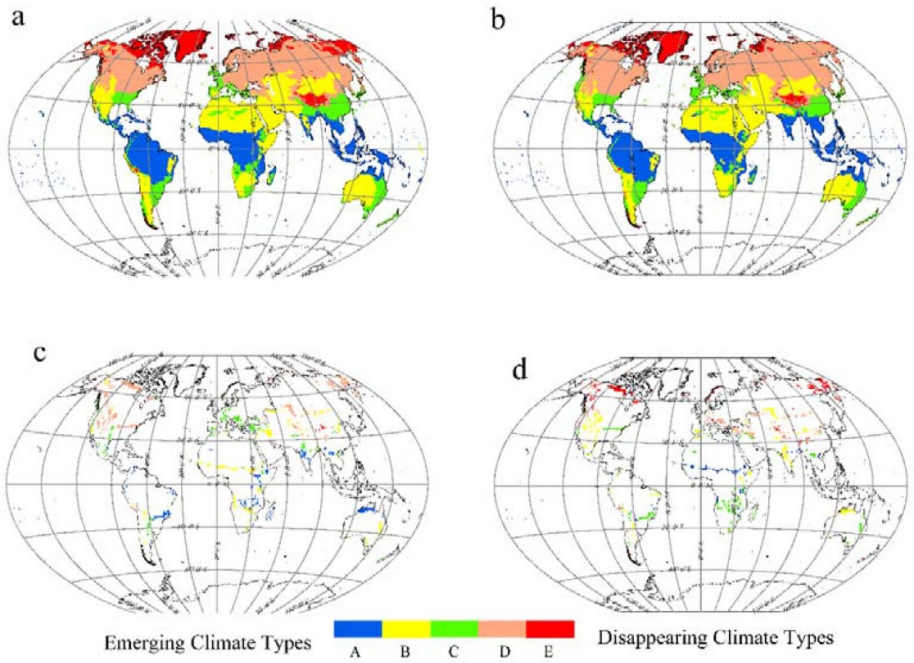


**Figure 1.** Distribution of the major climate types in (a) 1950 and (b) 2010, and the (c) 'emerging' and (d) 'disappearing' climate areas (zones shifting from one climate type to another); A to E represent tropical, arid, temperate, cold, and polar climates, respectively.

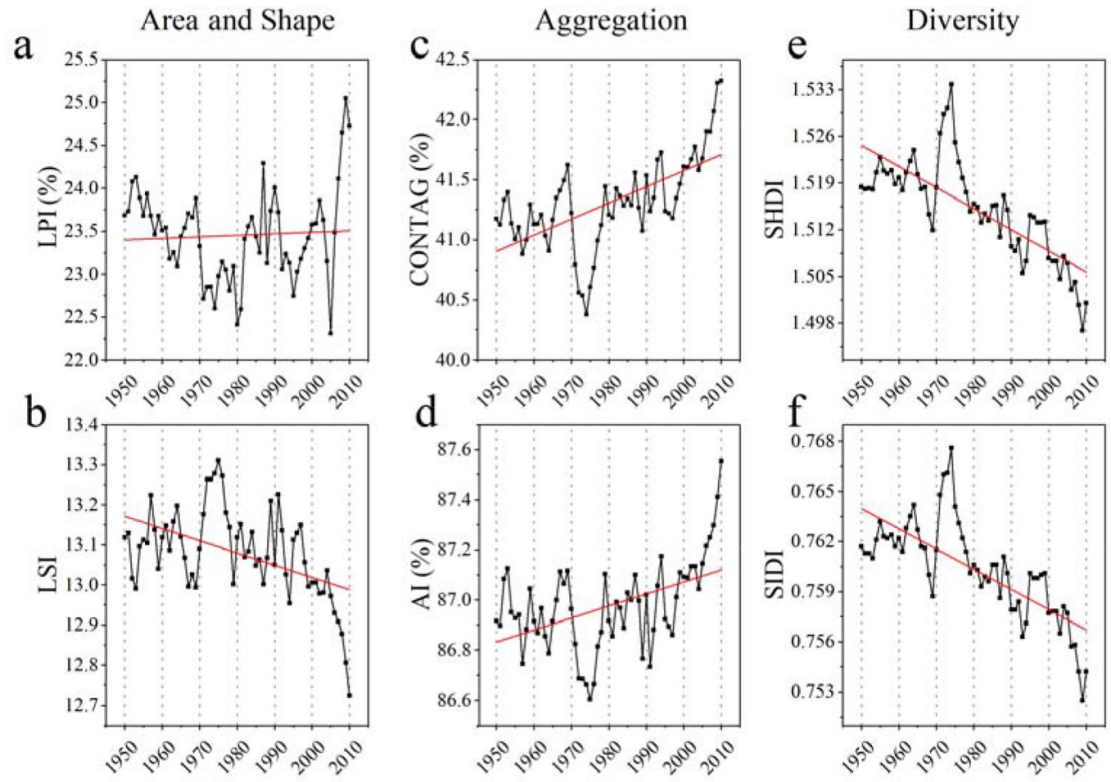


**Figure 2.** Changes in the climatic landscape indices from 1950 to 2010: (a) LPI, (b) LSI, (c) CONTAG, (d) AI, (e) SHDI, and (f) SIDI. The red line represents the linear trend of the variable.

the dispersion changes of the global climatic landscape. figure 4 reveals a strong correlation between the SD and landscape indices (all $p < 0.01$). When the SD anomaly grew by a rate of between −0.59 and 1.07, the LPI (figure 4(a)) increased from 23.68% to 24.73%, while the LSI (figure 4(b)) decreased from 13.12 to 12.72. At the same time, the CONTAG (figure 4(c)) and AI (figure 4(d)) variables increased

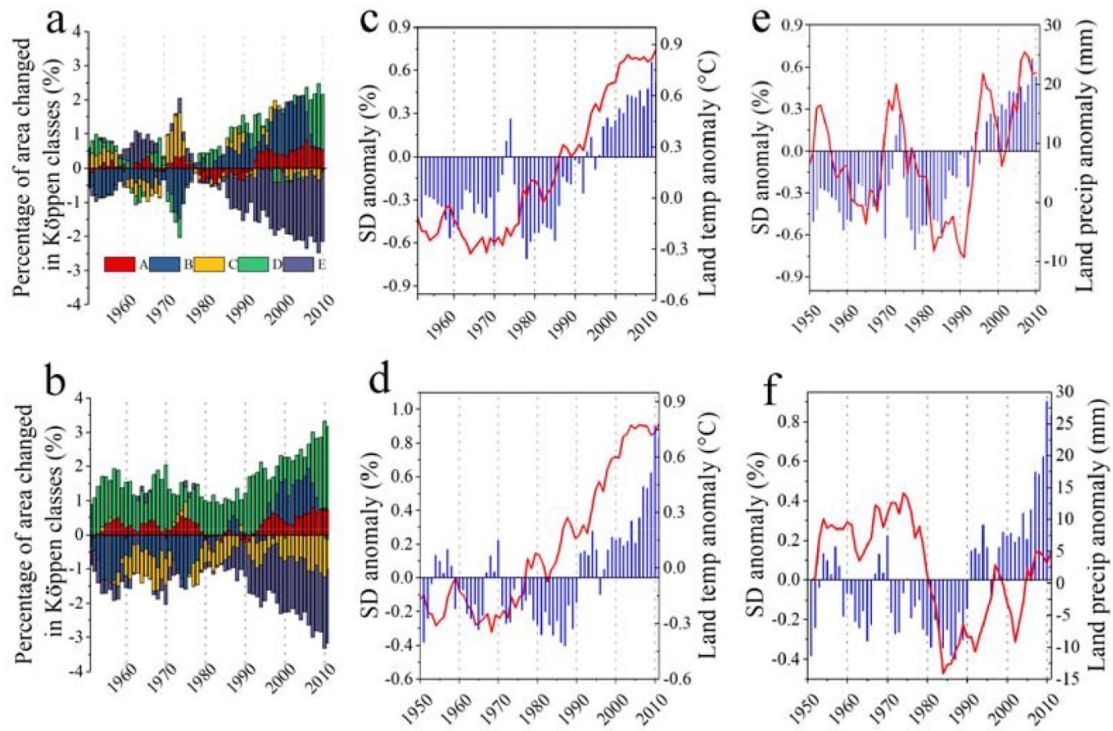


**Figure 3.** (a), (b) Cumulative changes in area in the Köppen climate classes in 1951–2010 relative to 1950. (c), (d) Anomalous changes in SD and surface temperature of the CRU and UD data, respectively. (e), (f) Anomalous changes in SD and surface precipitation of the CRU and UD data, respectively.

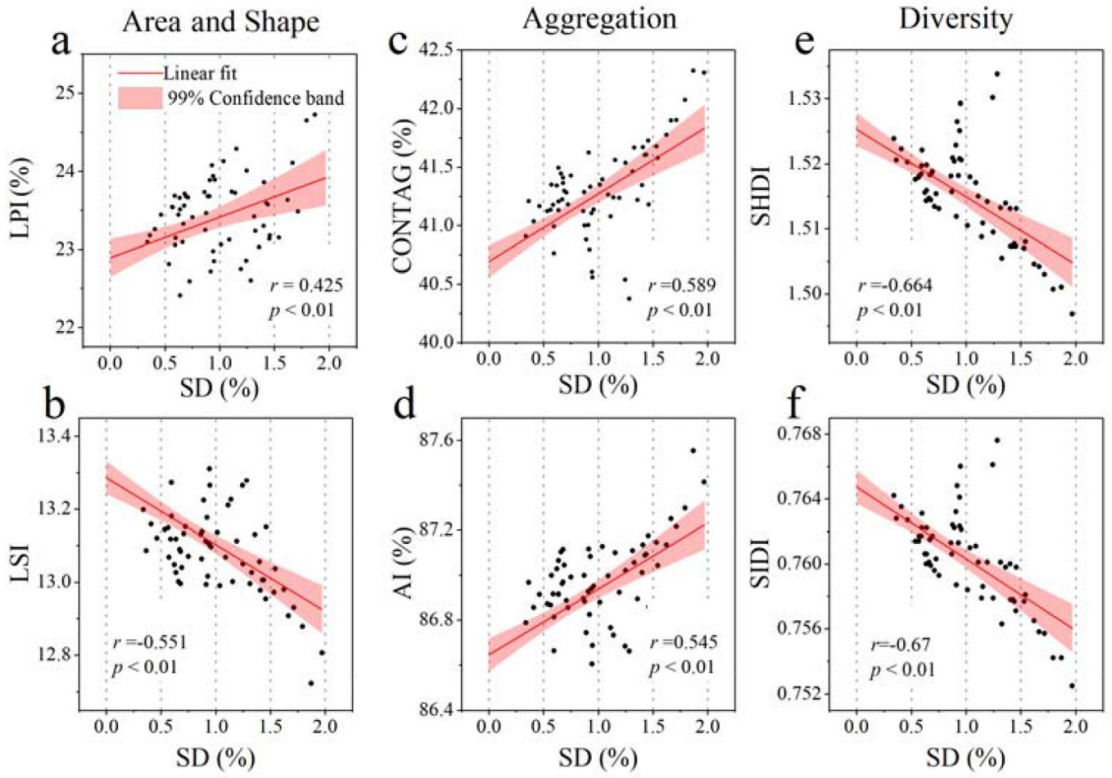


**Figure 4.** Correlation between the SD anomalies and (a) LPI, (b) LSI, (c) CONTAG, (d) AI, (e) SHDI, and (f) SIDI. *r* is the correlation coefficient, and *p* refers to the significance level (t-test).

significantly from 41.17 to 42.3 and 86.92 to 87.55, respectively, while the SHDI (figure 4(e)) and SIDI (figure 4(f)) indices decreased from 1.521 to 1.501 and 0.763 to 0.754, respectively. In summary, as the

SD rose, the area changed, the shape became more regular, the aggregation increased rapidly, and the climate diversity tended to decline, further suggesting that the dynamics of the SD are due to morphological variations in the global climatic landscape.

### 3.3. Landscape changes in continental climate pattern

To identify the regional climatic landscape characteristics, we mapped the continental distributions of major climatic zones and separately calculated the landscape indices relating to area (LPI), shape (LSI), aggregation (CONTAG & AI), and diversity (SHDI & SIDI; figures S2–13). The LPI (figure 5(a)) for all continents, excluding Europe, exhibited increasing trends ($-0.78\%$ decade$^{-1}$). For the LSI (figure 5(b)), increasing trends were observed in Africa (0.03 decade$^{-1}$), Australia ($0.2 \times 10^{-2}$ decade$^{-1}$), and Europe ($0.2 \times 10^{-2}$ decade$^{-1}$), while decreasing trends were observed in Asia, North America, and South America. Regarding aggregation (figures 5(c) and (d)), the trend of the CONTAG index increased in Africa, Asia, and South America, but decreased in Australia ($-0.2\%$ decade$^{-1}$), Europe ($-0.5\%$ decade$^{-1}$), and North America ($-0.13\%$ decade$^{-1}$), while the trend of the AI variable rose in Africa, Asia, South America, and North America and diminished rapidly in Australia ($-0.04$ decade$^{-1}$) and Europe ($-0.08$ decade$^{-1}$). The diversity trends (figures 5(e) and (f)) of SHDI and SIDI were similar, with decreases in Africa, Asia, Australia, and South America, and increases in Europe (0.01 decade$^{-1}$) and North America (0.06 decade$^{-1}$). Generally, in Europe and Australia, the changes in the aggregation variables have decreased, while the diversity is increasing in Europe and North America. However, in other continents, climatic landscapes are becoming more aggregated and climate diversity is decreasing.

## 4. Discussion

The SD index combines the changes in different climate zones as a whole, which greatly differs from other research, and changes in its value will cause a change in the morphology of major climate zones. Previous studies mainly concentrated on emerging and disappearing climates (Williams *et al* 2007, Burrows *et al* 2011), spatial changes to climatic types (Baker *et al* 2009, Rohli *et al* 2015a, Rubel *et al* 2017), the velocity at which these shifts occur (Mahlstein *et al* 2013, Chan and Wu 2015, Lu *et al* 2019), and the availability of different versions of world maps (Kottek *et al* 2006, Peel *et al* 2007, Kriticos *et al* 2012, Beck *et al* 2018). These studies are extremely important for understanding the climate, diagnosing climate change, and assessing their ecological impacts; however, the balance or complementary relationship between climate zones have been ignored. SD is calculated based on the complementary relationship of major climate zones, which may be a new indicator for evaluating global climate change. The SD index will continue to rise as the corresponding relationship of 'warm climates become larger and cold climates become smaller' continues, particularly under future warming scenarios (Taylor *et al* 2012).

Our results show that the aggregation of climatic patches in the global climate landscape has increased significantly, while climate diversity has declined. Given the lack of data on the distribution of species on Earth, most assessments of the impact of climate change on biodiversity have relied on simple climatic indicators that are often used to quantify the specific threats or opportunities for biodiversity (Ohlemüller *et al* 2008, Loarie *et al* 2009, Beaumont *et al* 2011, Sunday *et al* 2012, Watson *et al* 2013). As shifts in the biogeographic ranges of species have become one of the most direct biological responses to climate change (Burrows *et al* 2011), the morphological climatic measurements in the global climatic landscape are useful for understanding or predicting possible changes in the distribution of species (particularly poorly described or unknown species). For example, due to warmer temperatures, the alpine climates in major mountainous areas or polar climates will shrink and tropical or arid climates will expand (Kottek *et al* 2006, Allen *et al* 2012, Rohli *et al* 2015a, Rubel *et al* 2017), resulting in the aggregation of different climatic patches and a decrease in regional climate heterogeneity. Most climate niche models are based on the key assumption that climate distribution fundamentally determines the range of species (Pearson and Dawson 2003, Sunday *et al* 2012, Garcia *et al* 2014, Rohli *et al* 2015b, Beck *et al* 2018). Therefore, the aggregation process of climatic patches and the loss of climate diversity are highly likely to affect the availability and distribution of climatically suitable areas on a regional scale, resulting in changes in the seasonal activities (Lane *et al* 2012) of species living nearby or phenological shifts (Parmesan and Yohe 2003), such as flowering, migration, or breeding. This will potentially influence the demography and population dynamics of regional species and communities. Although climate landscape indices can be used to characterise changes in biodiversity, these changes are not equivalent to those in actual biomes. Thus, we must carefully consider and interpret the potential meaning of metric outputs.

Temporal climatic measurement scales are important. Changes measured over a long time often mask some important climatic signals of a finer temporal scale, thereby ignoring the measurement of climate change-related processes that may aid in understanding the contraction or expansion of the range of species. The Köppen-Geiger classification method using natural vegetation as a climatic expression aims to empirically determine the global distributions of

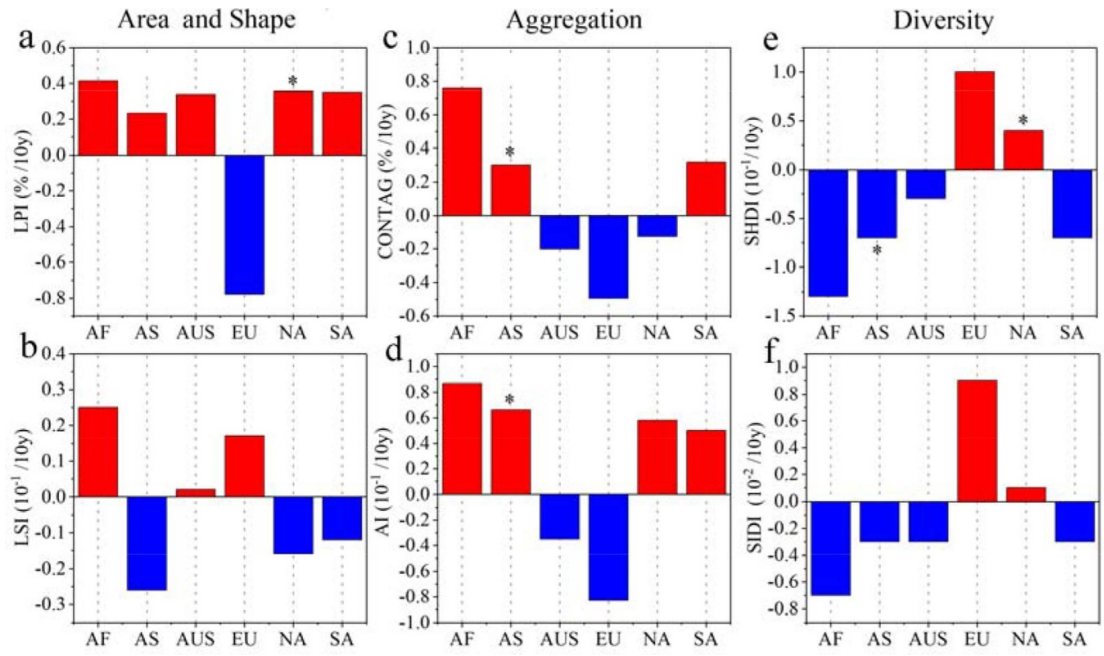


**Figure 5.** Linear trends of the LPI (a), LSI (b), CONTAG (c), AI (d), SHDI (e), and SIDI (f) of different continents, i.e. AF (Africa), AS (Asia), AUS (Australia), EU (Europe), NA (North America), and SA (South America). The asterisk denotes a 0.05 significance level ($|Z| > 1.96$, MK).

biomes. Due to the persistence of vegetation cover on multi-year scales, the long-term average climate distribution is more conducive to describing vegetation characteristics (Kottek *et al* 2006, Peel *et al* 2007, Beck *et al* 2018). However, the response of the spatial morphology is easier to observe on a finer temporal scale (such as interannual) than on a multi-year scale. The aggregation process and loss of climate diversity may cause a pronounced range of contraction for activities of species that depend on different climatic conditions at different life stages (such as seasonal migratory species), often mediating variations in their population demographics across seasons and lifespans.

Selecting an appropriate research scale depends on the questions and phenomenon being considered (Mcgarigal *et al* 2012), as the statistical relationship may change as the scale changes. Our statistical differences on the global and continental scales indicate that it is extremely important to consider climate change at different scales (Wu 2004, Chen *et al* 2017, Aalto *et al* 2018, Järvi *et al* 2019), as it may aid in our understanding of the climate itself. Similarly, the relatively coarse spatial resolution may limit the effectiveness of climatic assessments, which is insufficient to describe small-scale features, such as alpine tundra or frost climates (Rohli *et al* 2015b, Beck *et al* 2018). Rohli *et al* (2015b) found that the uncertainty caused by downscaling in some areas where stations are sparse limits the use of data with a finer resolution, especially in mountainous areas. (Beck *et al* 2018) systematically evaluated the accuracy and usability of the three latest versions of the Köppen-Geiger map, which has a relatively low resolution, and generated a new one with a resolution of 0.0083° that was is explicitly corrected for topographic effects. Furthermore, the demand information with a finer spatial resolution within the corresponding spatial range in landscape analysis is increasing (Buyantuyev and Wu 2007). From the landscape perspective, climate assessments at a lower spatial resolution may reduce regional climate diversity and ignore microrefugia (Garcia *et al* 2014), thereby overemphasising the risk to the survival of species survival at present ranges. Such climatic microrefugia patches with different climate conditions may allow species to persist and maintain their niche (Sunday *et al* 2011) during periods of climate change, particularly some poorly dispersed species (Williams *et al* 2007).

As global temperatures are likely to increase by at least 1.5 °C in the near future (Masson-Delmotte *et al* 2018), it is also necessary to explore the future potential evolution of the global Köppen-Geiger landscape under different emission pathways (Taylor *et al* 2012). The potential findings could provide more evidence to better understand future morphological changes of the climate and the implications for threats to and opportunities of biomes at different scales.

## 5. Conclusions

This research presents a quantification of shifts in the spatio-temporal patterns of major climate zones. Based on the area change of climate types on a zonal scale, SD index was used to characterize the dispersion

changes in major climate zones around the world, having the potential to be used as a new climate change indicator. Dispersion changes in area usually cause an overall change in spatial pattern. On this basis, changes in the morphology of global climatic landscape were effectively measured using different observed datasets. Our results indicate that there is a clear aggregation process of climatic patches, and a substantial decrease in climate diversity. These climatic morphological measurements are likely useful to interpret the specie's potential changes in demographic and mechanisms in response to climate change, such as seasonal activities or phenological shifts.

## Acknowledgments

We acknowledge NOAA/OAR/ESRL PSD, Boulder, Colorado, USA, for providing UD datasets on their Web site at www.esrl.noaa.gov/psd/, and also thanking Climatic Research Unit (CRU) for providing the high-resolution datasets, download from https://crudata.uea.ac.uk/cru/data/hrg/#current for providing. This work is funded by the Second Tibetan Plateau Scientific Expedition and Research Program (STEP), Grant No. 2019QZKK1003, the National Natural Science Foundation of China (Grant No. 41890824), the Strategic Priority Research Program of the Chinese Academy of Sciences (Grant No. XDA20040301) and the CAS Interdisciplinary Innovation Team (Grant No. JCTD-2019-04). 'Eduardo Maeda acknowledges funding from the Academy of Finland (decision numbers 318252 and 319905).' Furthermore, we would like to thank anonymous reviewers for their useful comments on the manuscript.

## Data availability

The data that support the findings of this study are available upon request from the authors.

## ORCID iDs

Yanlong Guan
https://orcid.org/0000-0001-9243-4073
Hari Adhikari
https://orcid.org/0000-0002-9089-3249
Eduardo Maeda
https://orcid.org/0000-0001-7932-1824

## References

Aalto J, Karjalainen O, Hjort J and Luoto M 2018 Statistical forecasting of current and future circum-Arctic ground temperatures and active layer thickness *Geophys. Res. Lett.* **45** 4889–98

Allen R J, Sherwood S C, Norris J R and Zender C S 2012 Recent Northern Hemisphere tropical expansion primarily driven by black carbon and tropospheric ozone *Nature* **485** 350–4

Almorox J, Quej V H and Martí P 2015 Global performance ranking of temperature-based approaches for evapotranspiration estimation considering Köppen climate classes *J. Hydrol.* **528** 514–22

Baker B, Diaz H, Hargrove W and Hoffman F 2009 Use of the Köppen-Trewartha climate classification to evaluate climatic refugia in statistically derived ecoregions for the People's Republic of China *Clim. Change* **98** 113–31

Beaumont L J, Pitman A, Perkins S, Zimmermann N E, Yoccoz N G and Thuiller W 2011 Impacts of climate change on the world's most exceptional ecoregions *Proc. Natl. Acad. Sci. U.S.A.* **108** 2306–11

Beck H E, Zimmermann N E, Mcvicar T R, Vergopolan N, Berg A and Wood E F 2018 Present and future köppen-geiger climate classification maps at 1-km resolution *Sci. Data* **5** 1–12

Boucher-Lalonde V, Morin A and Currie D J 2012 How are tree species distributed in climatic space? A simple and general pattern *Glob. Ecol. Biogeogr.* **21** 1157–66

Burrows M T *et al* 2011 The pace of shifting climate in marine and terrestrial ecosystems *Science* **334** 652–5

Buyantuyev A and Wu J 2007 Effects of thematic resolution on landscape pattern analysis *Landsc. Ecol.* **22** 7–13

Cain D H, Riitters K and Orvis K 1997 A multi-scale analysis of landscape statistics *Landsc. Ecol.* **12** 199–212

Carroll C, Parks S A, Dobrowski S Z and Roberts D R 2018 Climatic, topographic, and anthropogenic factors determine connectivity between current and future climate analogs in North America *Glob. Change Biol.* **24** 5318–31

Chan D and Wu Q 2015 Significant anthropogenic-induced changes of climate classes since 1950 *Sci. Rep.* **5** 1–8

Chen T, Zhang H, Chen X, Hagan D F, Wang G, Gao Z and Shi T 2017 Robust drying and wetting trends found in regions over China based on Köppen climate classifications *J. Geophys. Res.* **122** 4228–37

Feddema J J 2005 A revised thornthwaite-type global climate classification *Phys. Geogr.* **26** 442–66

Feng S, Hu Q, Huang W, Ho C H, Li R and Tang Z 2014 Projected climate regime shift under future global warming from multi-model, multi-scenario CMIP5 simulations *Glob. Planet. Change* **112** 41–52

Garcia R A, Cabeza M, Rahbek C and Araújo M B 2014 Multiple dimensions of climate change and their implications for biodiversity *Science* **344** 1247579

Greve P, Orlowsky B, Mueller B, Sheffield J, Reichstein M and Seneviratne S I 2014 Global assessment of trends in wetting and drying over land *Nat. Geosci.* **7** 716–21

Harris I, Jones P D, Osborn T J and Lister D H 2014 Updated high-resolution grids of monthly climatic observations - the CRU TS3.10 Dataset *Int. J. Climatol.* **34** 623–42

He H S, And B E D and Mladenoff D J 2000 An aggregation index (AI) to quantify spatial patterns of landscapes *Landsc. Ecol.* **15** 591–601

Järvi L, Havu M, Ward H C, Bellucco V, Mcfadden J P, Toivonen T, Heikinheimo V, Kolari P, Riikonen A and Grimmond C S B 2019 Spatial modeling of local-scale biogenic and anthropogenic carbon dioxide emissions in Helsinki *J. Geophys. Res. Atmos.* **124** 8363–84

Kendall M G 1975 *Rank Correlation Methods* (Griffin: London)

Knoben W J M, Woods R A and Freer J E 2018 A quantitative hydrological climate classification evaluated with independent streamflow data *Water Resour. Res.* **54** 5088–109

Kottek M, Grieser J, Beck C, Rudolf B and Rubel F 2006 World map of the Köppen-Geiger climate classification updated *Meteorol. Z.* **15** 259–63

Kriticos D J, Webber B L, Leriche A, Ota N, Macadam I, Bathols J and Scott J K 2012 CliMond: global high-resolution historical and future scenario climate surfaces for bioclimatic modelling *Methods Ecol. Evol.* **3** 53–64

Lane J E, Kruuk L E B, Charmantier A, Murie J O and Dobson F S 2012 Delayed phenology and reduced fitness associated with climate change in a wild hibernator *Nature* **489** 554–7

Lee J 1947 Determination of world plant formations from simple climatic data *Science* **105** 367–8

Liu C and Allan R P 2013 Observed and simulated precipitation responses in wet and dry regions 1850-2100 *Environ. Res. Lett.* **8** 034002

Loarie S R, Duffy P B, Hamilton H, Asner G P, Field C B and Ackerly D D 2009 The velocity of climate change *Nature* **462** 1052–5

Lu H, Guan Y, He L, Adhikari H, Pellikka P, Heiskanen J and Maeda E 2019 Patch aggregation trends of the global climate landscape under future global warming scenario *Int. J. Climatol.* **40** 2674–85

Mahlstein I, Daniel J S and Solomon S 2013 Pace of shifts in climate regions increases with global temperature *Nat. Clim. Change* **3** 739–43

Mann H B 1945 Nonparametric tests against trend *Econometrica: J. Econometric Soc.* **13** 245–59

Masson-Delmotte V, Zhai P, H-o P, Roberts D, Skea J, Shukla P R and Pirani A 2018 Global warming of 1.5 C *IPCC Spec. Rep. Impacts* www.climat.be/files/4115/3900/0027/181008_IPCC_sr15_spm.pdf

Mcgarigal K, Cushman S A and Ene E (2012). FRAGSTATS v4: spatial pattern analysis program for categorical and continuous maps Computer software program produced by the authors at the University of Massachusetts, Amherst (www.umass.edu/landeco/research/fragstats/fragstats.html)

Meybeck M, Kummu M and Dürr H H 2013 Global hydrobelts and hydroregions: improved reporting scale for water-related issues? *Hydrol. Earth Syst. Sci.* **17** 1093–111

O'Neill R V *et al* 1988 Indices of landscape pattern *Landsc. Ecol.* **1** 153–62

Ohlemüller R, Anderson B J, Araújo M B, Butchart S H M, Kudrna O, Ridgely R S and Thomas C D 2008 The coincidence of climatic and species rarity: high risk to small-range species from climate change *Biol. Lett.* **4** 568–72

Papagiannopoulou C, Miralles D G, Demuzere M, Verhoest N E C and Waegeman W 2018 Global hydro-climatic biomes identified via multitask learning *Geosci. Model Dev.* **11** 4139–53

Parmesan C and Yohe G 2003 A globally coherent fingerprint of climate change impacts across natural systems *Nature* **421** 37–42

Pearson R G and Dawson T P 2003 Predicting the impacts of climate change on the distribution of species: are bioclimate envelope models useful? *Glob. Ecol. Biogeogr.* **12** 361–71

Peel M C, Finlayson B L and Mcmahon T A 2007 Updated world map of the Köppen-Geiger climate classification *Hydrol. Earth Syst. Sci.* **11** 1633–44

Phillips T J and Bonfils C J W 2015 Köppen bioclimatic evaluation of CMIP historical climate simulations *Environ. Res. Lett.* **10** 064005

Pickett A S T A and Cadenasso M L 1995 Landscape ecology: spatial heterogeneity in ecological systems *Science* **269** 331–4

Rohli R V, Andrew Joyner T, Reynolds S J, Shaw C and Vázquez J R 2015a Globally extended Kppen-Geiger climate classification and temporal shifts in terrestrial climatic types *Phys. Geogr.* **36** 142–57

Rohli R V, Joyner T A, Reynolds S J and Ballinger T J 2015b Overlap of global Köppen–Geiger climates, biomes, and soil orders *Phys. Geogr.* **36** 158–75

Rubel F, Brugger K, Haslinger K and Auer I 2017 The climate of the European Alps: shift of very high resolution Köppen-Geiger climate zones 1800-2100 *Meteorol. Z.* **26** 115–25

Rubel F and Kottek M 2010 Observed and projected climate shifts 1901-2100 depicted by world maps of the Köppen-Geiger climate classification *Meteorol. Z.* **19** 135–41

Santini M and Di Paola A 2015 Changes in the world rivers' discharge projected from an updated high resolution dataset of current and future climate zones *J. Hydrol.* **531** 768–80

Senf C and Seidl R 2018 Natural disturbances are spatially diverse but temporally synchronized across temperate forest landscapes in Europe *Glob. Chang. Biol.* **24** 1201–11

Shannon C E 1948 A mathematical theory of communication *Bell Syst. Tech. J.* **27** 623–56

Simpson E H 1949 Measurement of diversity [16] *Nature* **163** 688

Sinervo B *et al* 2010 Erosion of lizard diversity by climate change and altered thermal niches *Science* **328** 894–9

Spinoni J, Vogt J, Naumann G, Carrao H and Barbosa P 2015 Towards identifying areas at climatological risk of desertification using the Köppen-Geiger classification and FAO aridity index *Int. J. Climatol.* **35** 2210–22

Sunday J M, Bates A E and Dulvy N K 2011 Global analysis of thermal tolerance and latitude in ectotherms *Proc. R. Soc.* B **278** 1823–30

Sunday J M, Bates A E and Dulvy N K 2012 Thermal tolerance and the global redistribution of animals *Nat. Clim. Change* **2** 686–90

Taylor K E, Stouffer R J and Meehl G A 2012 An overview of CMIP5 and the experiment design *Bull. Am. Meteorol. Soc.* **93** 485–98

Thornthwaite C W 1948 An approach toward a rational classification of climate *Geogr. Rev.* **33** 233–55

Thornthwaite C W 1961 The task ahead *Ann. Assoc. Am. Geogr.* **51** 345–56

Watson J E M, Iwamura T and Butt N 2013 Mapping vulnerability and conservation adaptation strategies under climate change *Nat. Clim. Change* **3** 989–94

Wells N, Goddard S and Hayes M J 2004 A self-calibrating Palmer Drought Severity Index *J. Clim.* **17** 2335–51

Williams J W, Jackson S T and Kutzbach J E 2007 Projected distributions of novel and disappearing climates by 2100 AD *Proc. Natl. Acad. Sci. U. S. A.* **104** 5738–42

Willmott C and Matsuura K 2001 *Terrestrial Air Temperature and Precipitation: Monthly and Annual Time Series (1950–1999) Version 1.02* (Newark: Center for Climatic Research, University of Delaware) (http://climate.geog.udel.edu/~climate/html_pages/README.ghcn_ts2.html.)

Wu J 2004 Effects of changing scale on landscape pattern analysis: scaling relations *Landsc. Ecol.* **19** 125–38

Yue S, Pilon P, Phinney B and Cavadias G 2002 The influence of autocorrelation on the ability to detect trend in hydrological series *Hydrol. Process.* **16** 1807–29